Association of Metallurgical Engineers of Serbia *Scientific paper*
AMES *UDC: 669.715*

MICROSTRUCTURE AND IMPRESSION CREEP CHARACTERISTICS AL-9SI-XCU ALUMINUM ALLOYS

MohsenYousefi*[1], Mehdi Dehnavi[2], S.M. Miresmaeili[1]

1 Department of Mechanical Engineering, Shahid Rajaee Teacher Training University, Tehran, Iran
2 Department of Materials Science and Engineering, Faculty of Engineering, Ferdowsi University of Mashhad, Iran

Received 17.09.2014
Accepted 26.03.2015

Abstract

The effects of 1.5, 2.5 and 3.5 wt.% Cu additions on the microstructure and creep behavior of the as-cast Al-9Si alloy were investigated by impression tests. The tests were performed at temperature ranging from 493 to 553 K and under punching stresses in the range 300 to 414 MPa for dwell times up to 3000 seconds. The results showed that, for all loads and temperatures, the Al–9Si–3.5Cu alloy had the lowest creep rates and thus, the highest creep resistance among all materials tested. This is attributed to the formation of hard intermetallic compound of Al_2Cu, and higher amount of α-Al_2Cu eutectic phase. The stress exponent and activation energy are in the ranges of 5.2- 7.2 and 115 -150 kJ/ mol, respectively for all alloys. According to the stress exponent and creep activation energies, the lattice and pipe diffusion- climb controlled dislocation creep were the dominant creep mechanism.
Keywords: Al-9Si alloy, Impression creep , Microstructure, Climb controlled dislocation creep.

Introduction

Among the Al based casting alloys, Al−Si−Cu alloys are the most widely used alloys in aerospace and automotive industries because of the good casting properties accompanied by the superior mechanical properties [1]. Based on the aluminum-silicon (Al-Si) system, the alloy contains copper and magnesium as the main alloying elements. Addition of Cu to eutectic Al-Si alloys leads to a slight increase in the alloy fluidity, and a depression in the Si eutectic temperature of ~1.8 K for every 1 wt.% Cu added. Also, some of the mechanical properties obviously benefit from the addition of Cu as an alloying element [2]. It is well known that at ~821 K, the amount of Cu in solid solution

* Corresponding author: MohsenYousefi, mo_metall80@yahoo.com

in Al is about 5.7 wt.% This value decreases with decreasing temperature, reaching 0.1– 0.2 wt.% at 523 K [3]. Copper forms an intermetallic phase with Al that precipitates during solidification either as block-like $CuAl_2$ or in eutectic form as $Al+CuAl_2$. In Al-Si-Cu alloys, the copper intermetallic phase precipitates in these two forms, according to a multicomponent eutectic reaction reported by Mondolfo [4]:

$$L \rightarrow Al+CuAl_2+\beta\text{-}Al_5FeSi+Si \quad (1)$$

Iron (Fe) is one of the most critical alloying elements for Al-Si-Cu alloys. During solidification, it forms several intermetallic compounds. Among these, the formation of hard brittle plates of the β-Al_5FeSi phase is particularly deleterious to the alloy mechanical properties [5]. In the recent years, many efforts have been carried out to enhance the high-temperature properties of aluminum alloys improving their application at that temperature [6]. Determining the dominant creep mechanism is the key factor for developing the alloys having high temperature mechanical properties [7,8]. Although the traditional tensile creep test is the common test for studying creep properties of materials, problems like cost of preparing standard samples, lack of microstructure uniformity and long test periods have limited the application of this method. Therefore, the studies have been conducted on using impression creep test during recent decades [9-13].

In contrast to conventional creep tests, which need tensile or compressive specimens, in this method, all creep data can be obtained with a small piece of material. Another advantage of this kind of test is that a constant stress can be attained during the entire creep test period[14]. Considering the aforementioned advantages, impression creep technique has been used in many researches to study creep properties of alloys [15,16]. Although impression creep technique has frequently been used for investigating creep properties of materials, it has not been standardized so far. It has been reported in many investigation that there is a good correspondence with results of both impression creep technique and those obtained from uniaxial tensile creep test [17,18]. Many investigations have been carried out on the impression creep properties of magnesium alloys, but impression creep properties of aluminum alloys have not been yet reported in the literature. Therefore, the aim of current research is to investigate the impression creep properties of Al-Si-Cu alloys.

Experimental Procedure

This investigation involved four alloys with the nominal chemical compositions of Al-9Si-xCu (x = 0, 1.5, 2.5, and 3.5 wt .%). The alloys were melted in a graphite crucible placed in an electrical furnace. Casting was poured at 1023 ± 5 K in a graphitic mold with dimensions of 120 × 40 × 10 mm, preheated up to about 473K. Then, samples with dimension of 10 × 10 × 6 mm were cut from the cast specimens by electro discharge wire cut machine. The creep tests were carried out using impression creep technique, in which a cylindrical indenter is impressed on the sample and the depth of penetration is monitored as a function of time. Some information about the impression creep test has been reported in the literature [19]. In the present investigation, a tungsten carbide indenter of 2 mm diameter was used and the tests were conducted in air in the temperature range of 493 to 553 K and under punching stresses in the range 300 to

414 MPa for about 3000 seconds. The samples for microstructure investigation were prepared by usual standard grinding and polishing methods. Etching was carried out using 0.5% HF solution at room temperature. Microstructural characterizations were examined by an Olympus BX60 optical microscope (OM) and a LEO-1550 scanning electron microscope (SEM). Energy-dispersive spectroscopy (EDS) analysis was carried out on selected samples to identify the phases.

Results and Discussions

Optical images of the investigated alloys are shown in Fig. 1. It can be seen that for base alloy, typical microstructure consists of the α-Al phase and Al-Si eutectic. The microstructure of the Al-9Si alloys contains Cu, α-Al phase, Al-Si eutectic and Cu-rich phases that are formed due to addition of Cu to the base alloy (Fig. 1b-d). The Cu enriched phases have been mainly distributed in the interdendritic regions and grainboundary. These phases are in the form of eutectic form as $Al+Al_2Cu$. Foramation of the Cu-rich phases in the microstructure depends on the amount of Cu in the (Fig. 1b-d). alloy and by increasing Cu content from 1.5 to 3.5 wt.%, volume fraction of these phases will increase (Table 1). In other hand, increasing Cu content decreases the stacking fault energy and these are the two main factors improving the creep behavior of the alloys containing Cu compared to the base alloy. Table 1. shows the quantification results of the Cu-rich phases formed in the investigated alloys.

Table 1. Average amount of Al_2Cu phase in the tested materials.

Alloy	Al_2Cu Phase (wt.%)
Al-9Si	0
Al-9Si-1.5Cu	1.7
Al-9Si-2.5Cu	2.4
Al-9Si-3.5Cu	4.3

In order to clarify the presence of alloying elements in the microstructure, distribution map of the alloying element of Al–9Si and Al–9Si–2.5Cu alloys are shown in Figs. 2 and 3, respectively. These Figures show that Fe is recognized in addition to the main alloying elements. Fe is present in all alloys as an impurity and because of its insolubility in the solid aluminum and formation of Fe-rich intermetallic compounds, should be maintained at the minimal possible amount. SEM image with EDS results of Al-9Si-2.5Cu alloy are shown in Fig. 4. As the results show, Cu and Fe rich phases are observed in the microstructure. Fe-rich compounds are usually in the form of β-Al_5FeSi platelets in the matrix, decorated by the $Al+CuAl_2$ eutectic.

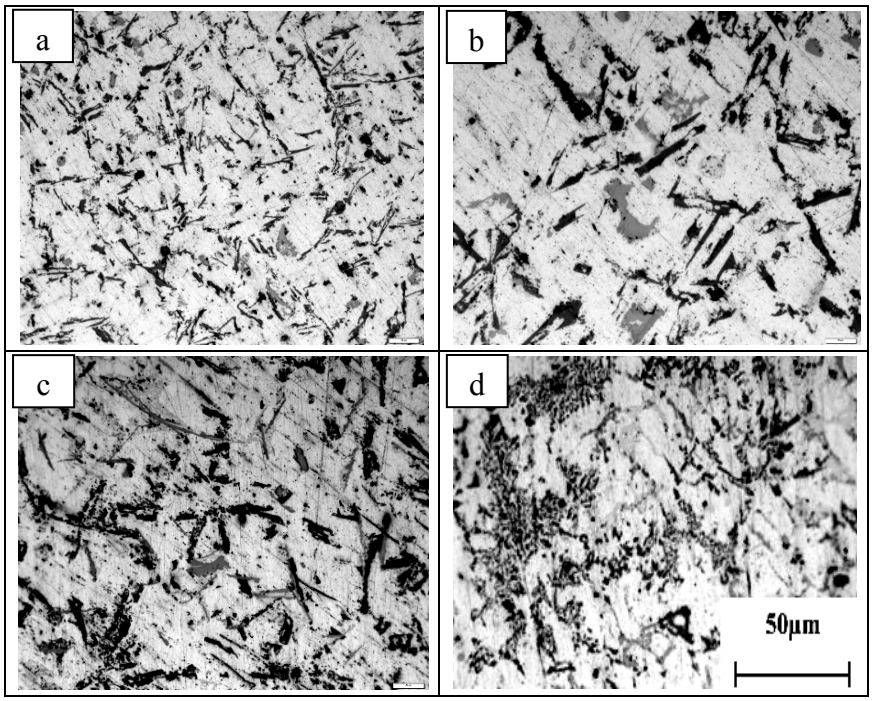

Fig. 1. Optical micrographs of (a) Al-9Si, (b) Al-9Si–1.5Cu, (c) Al-9Si–2.5Cu and (d) Al-9Si–3.5Cu alloy.

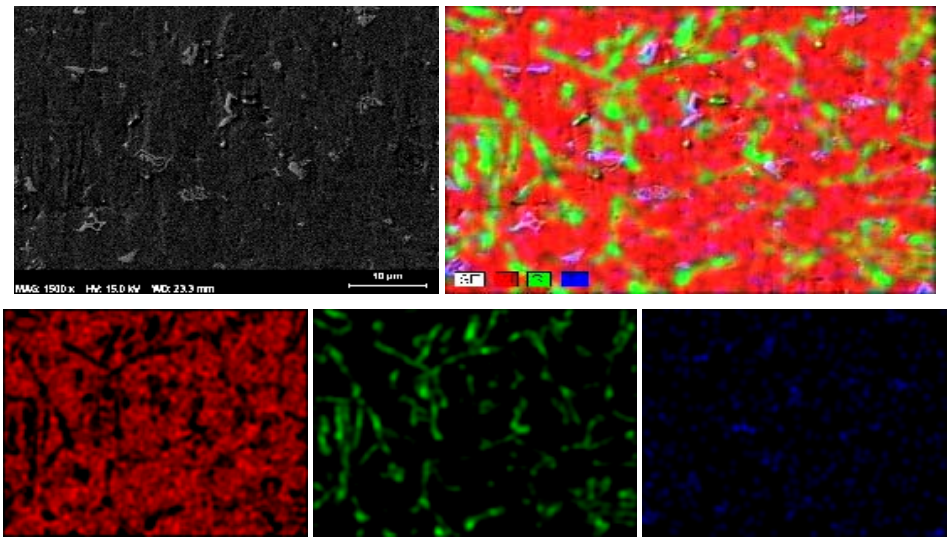

Al-KA *Si-KA* *Fe-KA*

Fig. 2. EDS elemental maps of Al-9Si alloy.

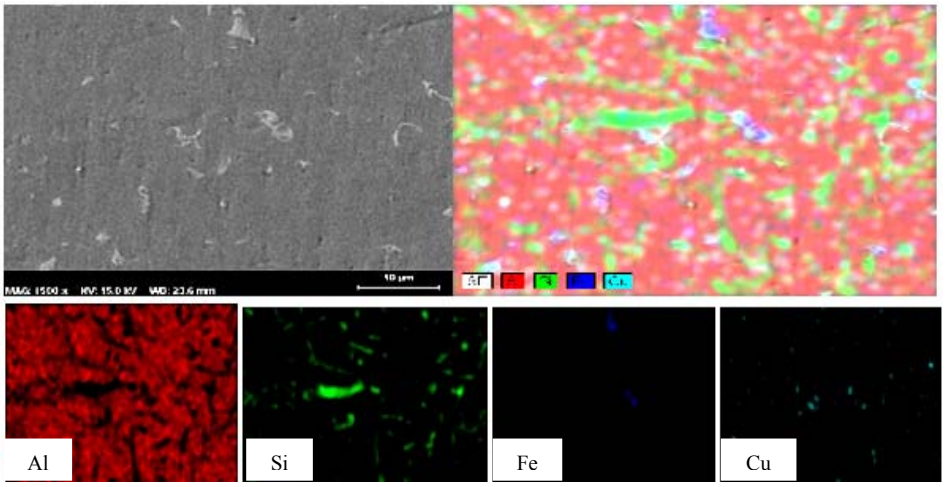

Fig. 3. EDS elemental maps of Al-9Si-2.5Cu alloy.

Impression creep behavior

Impression creep tests were performed under constant stress levels in the range 300–414 MPa, and in the temperature range 493–553 K. Typical impression depth–dwell time curves of all tested materials at 513 K under different punching stresses are shown in Fig. 5. These curves show that increasing stress at a constant temperature results in higher penetration rates. As can be seen, although each of the individual impression curves does not always exhibit a pronounced primary creep stage, they all eventually show a relatively long secondary or steady-state region where depth increases linearly with time. Since the impression test is actually a compression test, fracture of the specimen does not occur and hence, it is obviously not possible to record a third stage of the curve, as opposed to what occurs in an ordinary creep test. To be sure about the reproducibility of the impression creep data, at least three separate tests were taken at random places on the surface of the specimens for each condition and the creep curves were almost the same.

Concerning the reliability of the impression creep data, at least two separate measurements were taken at random places on the surface of the specimens for each condition and the creep curves were almost identical. A comparison on of the creep resistance of the investigated alloys at 533 K is depicted in Fig. 6. As can be inferred from this Figure, the Cu added Al-9Si alloys exhibit relatively higher creep resistances than that of the base alloy. This is evident from the slopes of the creep curves of Al–9Si–3.5Cu, as compared to other materials. The better creep resistance of the Al–9Si–3.5Cu alloy can partly be attributed to the higher volume fraction of the Al_2Cu phase with a high melting point of T_m=963K and high hardness. Furthermore, as discussed in the previous section, the Al_2Cu intermetallic particles are distributed in the grain boundary areas. Therefore, they can enhance the strength of the grain boundaries, by inhibiting their migration or sliding during diffusional creep.

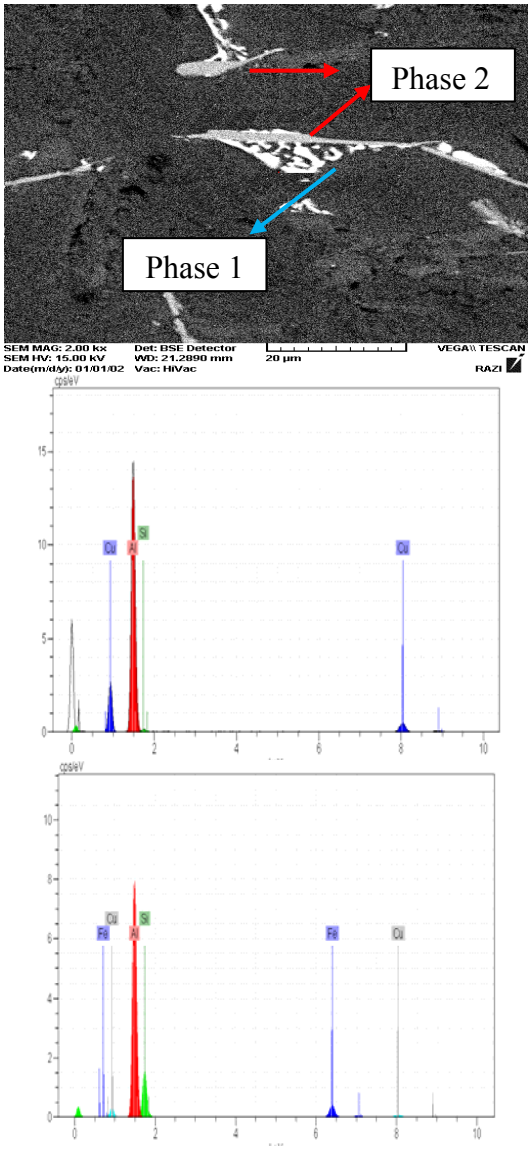

Fig. 4. SEM image of Al–9Si–2.5Cu alloy and EDS analysis of the β-Al_5FeSi platelet (phase 2), and eutectic Al+$CuAl_2$ (phase 1).

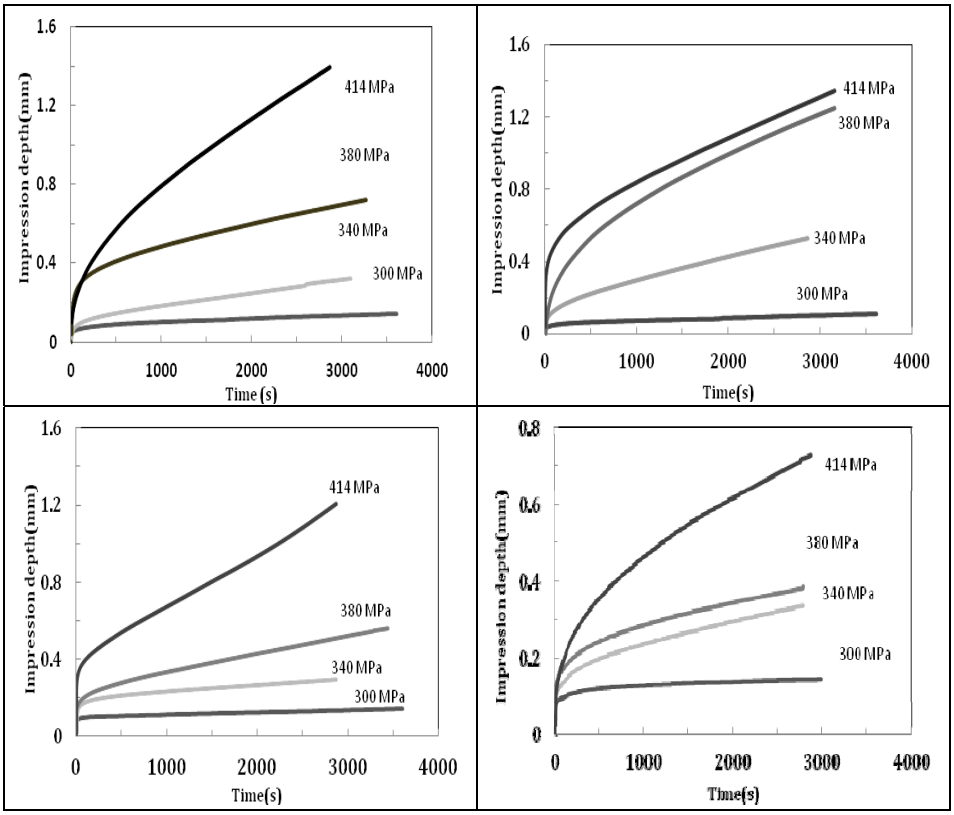

Fig. 5. Typical creep curves of the investigated alloys at 513 K under different stress levels: (A) Al-9Si, (B) Al– 9Si–1.5Cu, (C) Al–9Si–2.5Cu and (D) Al–9Si–3.5Cu alloy.

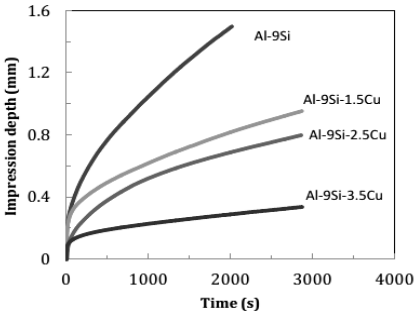

Fig. 6. Variations of impression depth versus time of the investigated alloys at 533 K.

Creep mechanism

To determine the creep mechanism of metallic materials it is common to calculate the stress exponent (n) and activation energy (Q) by conducting a series of creep measurements at different temperatures and stresses. The stress dependence of the

steady-state creep rate is generally expressed by means of the power law equation as follows [20]:

$$\dot{\varepsilon} = A(\sigma_{imp})^n \exp\left(-\frac{Q}{RT}\right) \tag{2}$$

where A is a material parameter, σ_{imp} is the applied impression stress, n is the stress exponent, Q is the creep activation energy, T is the temperature, and R is the universal gas constant. To correlate impression and tensile creep data, equivalent stress and strain rate can be evaluated from the impression velocity (V_{imp}=dh/dt), the impression stress under the punch ($\sigma_{imp} = 4F/\pi\phi^2$) at a given load F and punch diameter ϕ as:

$$\sigma = \frac{\sigma_{imp}}{c_1} \quad \text{and} \quad \dot{\varepsilon} = \frac{dh/dt}{\phi c_2} = \frac{V_{imp}}{\phi c_2} \tag{3}$$

where c_1 and c_2 are constants. It has been shown experimentally that both stress and temperature dependencies of the steady-state impression velocity agree with the corresponding dependencies of the creep rate in conventional creep tests [21]. Therefore, inserting Eq.(2) into Eq.(1) and rearranging gives the relationship between impression velocity and applied punch stress. Accordingly:

$$V_{imp} = B(\sigma_{imp})^n \exp\left(-\frac{Q}{RT}\right) \tag{4}$$

Since B is a constant, it is possible to obtain the stress exponent n from a plot of ln (V_{imp}) against ln (σ_{imp}) at constant T. Similarly, the activation energy Q can be obtained from a plot of ln (V_{imp}) versus (1/T) at constant (σ_{imp}). As Eq. (1) reveals, the value of stress exponent n, demonstrating the creep mechanism is obtained from the slope of the variation of ln(v_{imp}) versus ln(σ) at constant temperature. Fig. 7. shows the variation of ln (V_{imp}) versus ln (σ_{imp}) at constant temperature.

Slope of the lines (n) also are shown in Fig.7. The n-value of Al–9Si is 7.1 at 493K, and 6.2 at 553K. As temperature rises from 493 K to 553 K, the stress exponent decreases, from 5.3 to 7.0, 5.3 to 6.9, and 5.6 to 7.2, for Al–9Si–1.5Cu, Al–9Si–2.5Cu and Al–9Si–3.5Cu, respectively. Obtained stress exponent values shown in Fig. 7. And compared with those reported in Ref. [22] indicate that the climb controlled dislocation creep is the dominant mechanism during creep of the all alloys.

Fig. 8. demonstrates the variation of ln (V_{imp}) versus 1/T under constant stresses The corresponding creep activation energies shown in Fig. 8 were obtained from the slope of the best-fit lines. It is observed that the average activation energy of the alloys varies between 116 kJ/mol and 147 kJ/mol. The activation energies vary between that of aluminum pipe diffusion (82 kJ/mol) and lattice self-diffusion (142 kJ/mol) [23]. This implies that the dislocation climb velocity is controlled by two parallel mechanisms of aluminum diffusion in the lattice and dislocation pipe which take place simultaneously. In such a case it has been reported that one of the mechanisms is dominant. It is possible to determine the dominant creep mechanism by comparing creep activation energy with critical activation energy that above which the dominant mechanism is the lattice diffusion and below which pipe diffusion is the dominant mechanism [14,19].

According to Fig. 8, values of the activation energy decrease with punching stress. This can be attributed to the presence of higher density of dislocation in the

specimens crept under higher stresses. In fact, the rate of dislocation production increases with stress resulting in higher dislocation density. By increasing the dislocation density, the rate of materials flow by diffusion in the dislocation pipe will be higher than that through the lattice which leads to the lower activation energy. Creep improvement during dislocation climb controlled creep may is controlled by two factors: 1) higher amount of intermetallic components between the grains and interdendritic regions; 2) decrease of stacking fault energy of the matrix phase by increases of Cu content. The higher amount of intermetallic compounds increases the creep properties by reducing annihilation of dislocations in the grain boundaries and by decreasing grain boundary sliding. The distance between partial dislocations increases by decreasing stacking fault energy, resulting in the difficulty of dislocation climbing. In such cases, greater stress is needed for dislocations with o combine each other and climb overthe obstacles. The amount of Cu dissolved in α(Al) phase increases with increasing of Cu. Therefore, it seems that Cu reduces stacking fault energy of α(Al) phase, resulting in the increased creep properties [24]. Because of more dissolved Cu in α(Al) phase of Al–9Si–3.5Cu alloy compared to the other alloys, more reduction in stacking fault energy occurs in Al–9Si–3.5Cu alloy. Therefore, Al–9Si–3.5Cu alloy exhibits better creep resistance in comparison with other alloys.

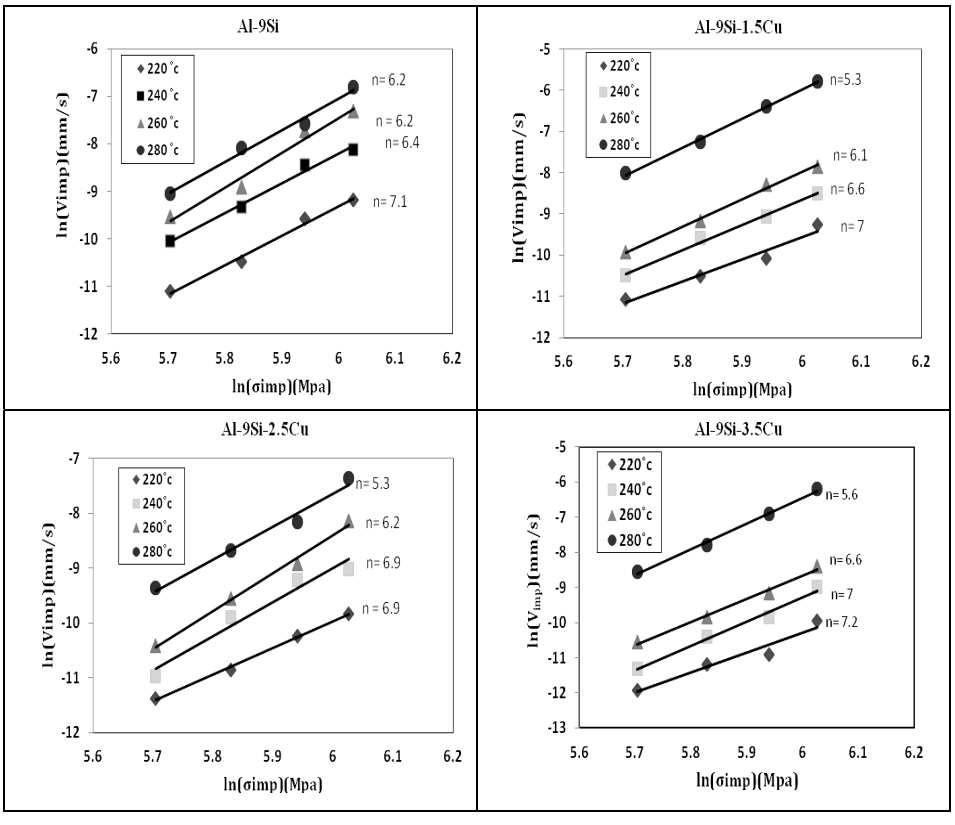

Fig. 7. Variations of ln (V_{imp}) vs. ln (σ_{imp}) at constant temperatures .

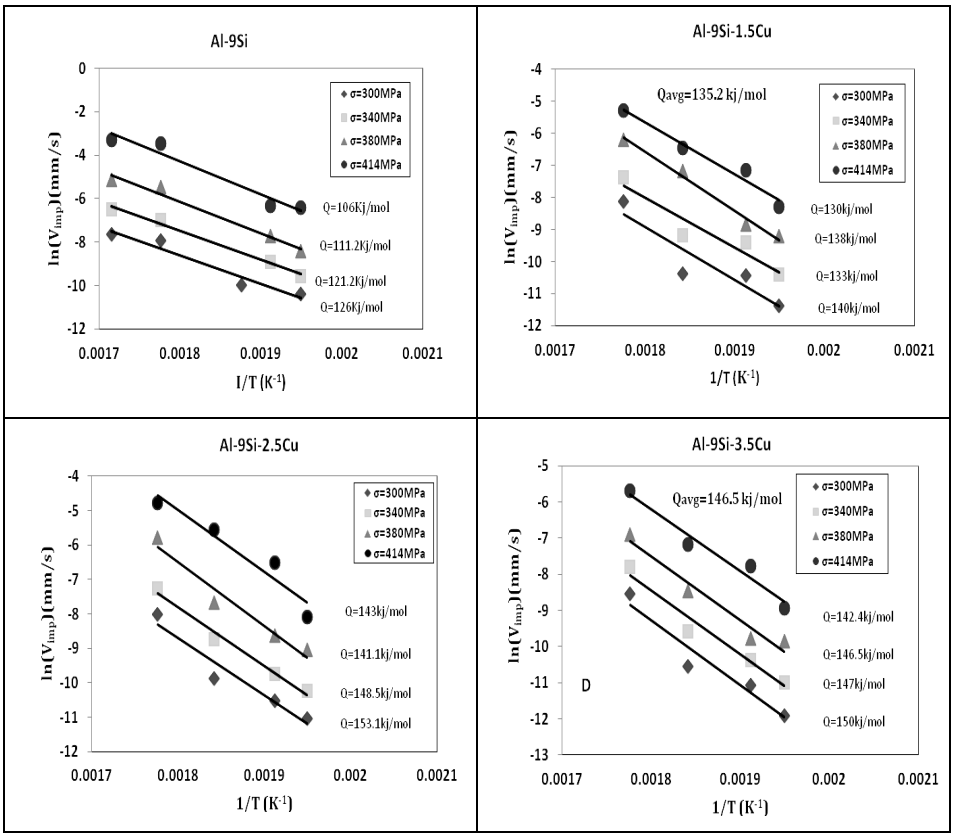

Fig. 8. Variations of ln (V_{imp}) vs. 1/T under constant stresses.

Conclusions

Effect of Cu on microstructure and impression creep properties of Al-9Si alloy in the temperature range 493–553 K under stress levels in the range 300–414 MPa were investigated. The following results were obtained:

1. The microstructure of the investigated alloys consists of the α-Al phase, Al-Si eutectic and Al+$CuAl_2$ eutectic.
2. The Cu enriched phases are mainly distributed in the interdendritic regions and these phases affect on a significant enhancement in creep resistance.
3. The values of the obtained stress exponent indicate that climb controlled dislocation creep is the dominant creep mechanism.
4. The average activation energy of the alloys varies between 116 kJ/mol and 147 kJ/mol . These values indicate indicates that the velocity of dislocation climb is controlled by diffusion of Al atoms through the dislocation pipe and lattice. Therefore, it can be concluded that under the conditions used in the present study, lattice and pipe diffusion climb controlled dislocation creep are the main creep mechanism which influencing the creep rate of the alloys.

References

[1] J. E. Hatch, American Society for Metals, Metals Park, OH, (1984) 143.
[2] M. A. Moustafa, F. H. Samuel, H. W. Doty, S. Valtierr A, Int. J. Cast Metals Res14 (2002) 235-40
[3] M. Hansen,"Constitution of Binary Alloys", 2nd ed. (McGrawHill, New York, 1958) pp. 84.
[4] L. F. Mondolfo, Butterworths, London, (1976).
[5] Z. Li, A. M. Samuel, F. H. Samuel, J. Mat.Sci 38 (2003)1203 – 1218.
[6] L. Peng, F. Yang, J. Nie, Mater. Sci. Eng A 410 (2005) 42–7
[7] K. Milicka, P. Perez, F. Dobes, G. Garces, P. Adeva, Mater. Sci. Eng A 510-511 (2009) 377–81.
[8] J. Guo, L. Chen, Y. Xu, F. Lian, Mater. Sci. Eng A 443(2007) 66–70.
[9] B. Nami, H. Razavi, S.M. Miresmaeili, Sh. Mirdamadi, S.G. Shabestari, Scripta Mater 65 (2001) 221–4.
[10] PM. Sargent, MF. Ashby, Mater. Sci. Technol 8 (1992) 594–601.
[11] R. Mahmudi, AR. Granmayeh, M. Bakherad, M. Allami, Mater. Sci. Eng A 457 (2007) 173–9.
[12] Chu SNG, Li JCM, Mater. Sci 12 (1977) 2200–8.
[13] DH. Sastry, Mater. Sci. Eng A 409 (2005) 67–75.
[14] F. Kabirian, R .Mahmudi, Met. Mater. Trans A 40 (2009) 116–27.
[15] B. Nami, SG. Shabestari, SM. Miresmaeili, H. Razavi, Sh. Mirdamadi, J Alloys Compd 489 (2010) 570–5.
[16] N. Kashefi, R. Mahmudi, Mater Des 39 (2012) 200–10.
[17] AK .Mondale, S .Kumar, Compos Sci Technol 68 (2008) 3251–8.
[18] B. Kondori, R. Mahmudi, Met. Mater. Trans A 40 (2007) 2007–15.
[19] B. Nami, H. Razavi, S. Mirdamadi, SG. Shabestari, SM. Miresmaeili, Met. Mater. Trans A (2010)1973–82
[20] A.K. Mukherjee, J.E. Bird, J.E. Dorn, Trans. ASM 62 (1969) 155–179.
[21] R. Mahmudi, A. Karsaz, A. Akbari-Fakhrabadi, A.R. Geranmayeh, Mater. Sci. Eng A 527 (2010) 2702–2708.
[22] H. Somekawa, K. Hirai, H. Watanabe, Y. Takigawa, K. Higashi Mater. Sci. Eng A 407 (2005) 53–61.
[23] HJ. Frost, MF. Ashby, New York, Pergamon Press (1982).
[24] B. Amir esgandari, B. Nami, M. Shahmiri, A. Abedi, Trans. Nonferrous Met. Soc. China 23(2013) 2518−2523.